ELSEVIER

Materials Chemistry and Physics 61 (1999) 207–213

MATERIALS CHEMISTRY AND PHYSICS

www.elsevier.com/locate/matchemphys

Thermal stresses due to spheroidal inclusions

Sanboh Lee[a,*], P.K. Liaw[b], C.T. Liu[c], Y.T. Chou[a,1]

[a]Department of Materials Science, National Tsing Hua University, Hsinchu, Taiwan

[b]Department of Materials Science and Engineering, University of Tennessee, Knoxville, TN 37996-2200, USA

[c]Metals and Ceramics Division, Oak Ridge National Laboratory, Oak Ridge, TN 37831-6115, USA

Received 23 February 1999; received in revised form 30 April 1999; accepted 14 May 1999

Abstract

Thermal stresses due to a spheroidal inclusion were investigated using the equivalent inclusion approach proposed by Eshelby. The temperature inside the spheroid is maintained constant and different from that of the surrounding matrix of an infinite extent. A new relation between the Cartesian coordinates and spheroidal coordinates was established. Based on this relation, the solution for a prolate spheroidal inclusion was readily obtained from that for an oblate spheroidal inclusion. The principal stress inside the spheroid increases with decreasing m, the ratio of shear moduli of the spheroid and matrix. The value of σ_{11}^{I} inside the spheroid increases with increasing k, the aspect ratio, but the trend for σ_{33}^{I} is opposite. The stress components, σ_{11}, along the x_1 axis and, σ_{33}, along the x_3 axis in the matrix decrease with increasing distance away from the inclusion. For given combinations of m and k, the maximum stress components, σ_{22} and σ_{33}, along the x_1 axis and σ_{11} $(= \sigma_{22})$ along the x_3 axis in the matrix are located at certain distances away from the interface. Among all principal stresses, the maximum tensile stress is located at the interface between the inclusion and matrix. The numerical results are in agreement with those reported in the literature. © 1999 Elsevier Science S.A. All rights reserved.

Keywords: Thermal stresses; Oblate spheroidal inclusion; Prolate spheroidal inclusion

1. Introduction

Eshelby [1,2] proposed an equivalent inclusion method to solve the stress distribution inside and outside a spheroidal inhomogeneity. The spheroidal inhomogeneity is referred to a system in which the elastic constants of the spheroidal inclusion are different from those of the matrix. This method was also described in the book by Mura [3]. Sadowsky and Sternberg [4] solved the stress field of a prolate spheroidal cavity under remote loading based on an extension of orthogonal curvilinear coordinates of the classical three-function approach to three-dimensional problems in elasticity. Using the same method, Edwards [5] calculated the stress fields inside and outside a prolate spheroidal inhomogeneity under remote loading. Shibato and Ono analyzed the stress distribution due to a prolate spheroidal inclusion under an applied stress [6] and due to a misfit interface bounded by an oblate spheroidal inclusion and the matrix [7], based upon the Eshelby approach [1,2].

The stresses due to a mismatch in thermal expansion coefficients between the inclusion and infinite matrix have been extensively analyzed to understand fracture and mechanical strength of metal alloys and composites [8–12]. The elastic stresses due to a discontinuity in temperature in a system containing an oblate or prolate spheroid of the same material are given in the book by Nowacki [13]. Using a three function approach, Edwards [5] obtained the thermal stresses due to a prolate spheroidal inhomogeneity. In this paper, we solved the thermal stresses due to both prolate and oblate spheroidal inhomogeneities based on the equivalent inclusion method.

2. Stress analysis

As an introduction to our model, consider a spheroidal inhomogeneity in an infinite matrix subjected to a temperature change T. Both the spheroid and the matrix are assumed to be elastically isotropic, and their shear moduli and Poisson's ratios are denoted by μ^*, ν^* and μ, ν, respectively. The interface between the spheroid and matrix is assumed to be perfectly bonded. The spheroid in the Cartesian coordinate system, x_1, x_2, x_3, is defined by

*Corresponding author.

[1]On leave from the Department of Materials Science and Engineering, Lehigh University, Bethlehem, PA 18015, USA.

0254-0584/99/$ – see front matter © 1999 Elsevier Science S.A. All rights reserved.
PII: S0254-0584(99)00118-2

$$\frac{x_1^2+x_2^2}{a^2}+\frac{x_3^2}{c^2}\le 1 \tag{1}$$

The aspect ratio, k, is defined as c/a, and is greater than, equal to, and smaller than unity for a prolate spheroid, sphere, and oblate spheroid, respectively. The uniform strain arising from the temperature change, T, is

$$e_{11}^{\mathrm{P}}=e_{22}^{\mathrm{P}}=e_{33}^{\mathrm{P}}=(\alpha^*-\alpha)T \tag{2}$$

where α^* and α are the coefficients of thermal expansion of the spheroid and matrix, respectively.

The stress field is solved using the equivalent inclusion method proposed by Eshelby [1,2]. The internal stress σ_{ij}^{I} inside the spheroid is given by

$$\sigma_{ij}^{\mathrm{I}}=\lambda^*\delta_{ij}(e_{kk}^{\mathrm{C}}-e_{kk}^{\mathrm{P}})+2\mu^*(e_{ij}^{\mathrm{C}}-e_{ij}^{\mathrm{P}})=\lambda\delta_{ij}(e_{kk}^{\mathrm{C}}-e_{kk}^{\mathrm{T}})+2\mu(e_{ij}^{\mathrm{C}}-e_{ij}^{\mathrm{T}}) \tag{3}$$

where λ^* and λ are, respectively, the Lame's constants of the spheroid and matrix, and δ_{ij} is the Kronecker delta. Note that the Einstein summation convention is used throughout this paper. The constraint strain, e_{ij}^{C}, is related to the transformation strain e_{ij}^{T} by

$$e_{ij}^{\mathrm{C}}=S_{ijkl}e_{kl}^{\mathrm{T}} \tag{4}$$

with

$$S_{1111}=S_{2222}=\frac{3}{8(1-\nu)}\left[1-\frac{1+3M}{2(k^2-1)}\right]+\frac{1-2\nu}{4(1-\nu)}(1+M) \tag{5a}$$

$$S_{1122}=\frac{1}{8(1-\nu)}\left[1-\frac{1+3M}{2(k^2-1)}\right]-\frac{1-2\nu}{4(1-\nu)}(1+M) \tag{5b}$$

$$S_{1133}=S_{2233}=\frac{1}{4(1-\nu)}\frac{k^2(1+3M)}{k^2-1}-\frac{1-2\nu}{4(1-\nu)}(1+M) \tag{5c}$$

$$S_{3311}=S_{3322}=\frac{1+3M}{4(1-\nu)(k^2-1)}+\frac{(1-2\nu)M}{2(1-\nu)} \tag{5d}$$

$$S_{3333}=\frac{1}{2(1-\nu)}\left[1-\frac{k^2(1+M)}{k^2-1}\right]-\frac{(1-2\nu)M}{2(1-\nu)} \tag{5e}$$

$$M=\begin{cases}1/(k^2-1)-k/((k^2-1)^{3/2})\cosh^{-1}(k) & \text{for } k\ge 1\\ 1/(k^2-1)+k/((1-k^2)^{3/2})\cos^{-1}(k) & \text{for } k<1\end{cases} \tag{5f}$$

$$m=\frac{\mu^*}{\mu} \tag{5g}$$

and

$$e_{ij}^{\mathrm{T}}=\begin{pmatrix}e_{11}^{\mathrm{T}} & 0 & 0\\ 0 & e_{11}^{\mathrm{T}} & 0\\ 0 & 0 & e_{33}^{\mathrm{T}}\end{pmatrix} \tag{6}$$

In Eq. (4), S_{ijkl} is a dimensionless parameter. Lee et al. [14] reported that S_{ijkl} is proportional to the reciprocal of shear modulus. S_{3311} ($=S_{3322}$) is not equal to S_{1133} ($=S_{2233}$), but the authors treated both as the same quantity [14], that is, $S_{3311}=S_{1133}$.

Assuming $\nu=\nu^*$ and substituting Eq. (4) into Eq. (3), we obtain

$$e_{11}^{\mathrm{T}}=\frac{R-Q}{RP-QS}(1+\nu)m(\alpha^*-\alpha)T \tag{7a}$$

$$e_{33}^{\mathrm{T}}=\frac{P-S}{RP-QS}(1+\nu)m(\alpha^*-\alpha)T \tag{7b}$$

in which

$$P=2(m-1)[\nu(S_{1111}+S_{1122})+(1-\nu)S_{3311}]+2\nu \tag{8a}$$

$$Q=(m-1)[2\nu S_{1133}+(1-\nu)S_{3333}]+1-\nu \tag{8b}$$

$$R=(m-1)(S_{1133}+\nu S_{3333})+\nu \tag{8c}$$

$$S=(m-1)[S_{1111}+S_{1122}+2\nu S_{3311}]+1 \tag{8d}$$

The stresses inside the spheroid can be obtained from Eqs. (3), (7a) and (7b), and we have

$$\sigma_{11}^{\mathrm{I}}=\sigma_{22}^{\mathrm{I}}=\frac{2\mu(1+\nu)m(\alpha^*-\alpha)T}{(1-2\nu)(m-1)(RP-QS)}\{(S-m)(R-Q)+(R-\nu m)(P-S)\} \tag{9a}$$

$$\sigma_{33}^{\mathrm{I}}=\frac{2\mu(1+\nu)m(\alpha^*-\alpha)T}{(1-2\nu)(m-1)(RP-QS)}\{(P-2\nu m)(R-Q)+(Q-m+m\nu)(P-S)\} \tag{9b}$$

Two special cases are worthwhile to mention. First, when k approaches 0, the spheroidal inclusion reduces to a penny shape. The stresses inside the penny inclusion are

$$\sigma_{11}^{\mathrm{I}}=\sigma_{22}^{\mathrm{I}}=\frac{-2m\mu(1+\nu)(\alpha^*-\alpha)T}{1-\nu} \tag{9c}$$

$$\sigma_{33}^{\mathrm{I}}=0 \tag{9d}$$

Second, if k reaches infinity, the shape of inclusion becomes a circular cylinder. The stresses inside the circular cylinder are

$$\sigma_{11}^{\mathrm{I}}=\sigma_{22}^{\mathrm{I}}=\frac{-2m\mu(1+\nu)(\alpha^*-\alpha)T}{m+1-2\nu} \tag{9e}$$

$$\sigma_{33}^{\mathrm{I}}=\frac{-2m(1+m)\mu(1+\nu)(\alpha^*-\alpha)T}{m+1-2\nu} \tag{9f}$$

Fig. 1 (a) presents the relation between σ_{11}^{I} and m for various values of k. All curves are merging to the same line when $m<0.3$. For a given k, σ_{11}^{I} decreases rapidly with increasing m and then reaches a plateau. A similar trend is observed in the variation of σ_{33}^{I}, as shown in Fig. 1(b). For a given m, σ_{11}^{I} increases with increasing k, but σ_{33}^{I} is in the opposite trend. Note that a factor of 2 is missed in the denominator of the last term containing e^2, in the expression of σ_{33} in Eq. (17) of [13].

The stresses outside the spheroid can be obtained as follows. Assume the oblate spheroid coordinates

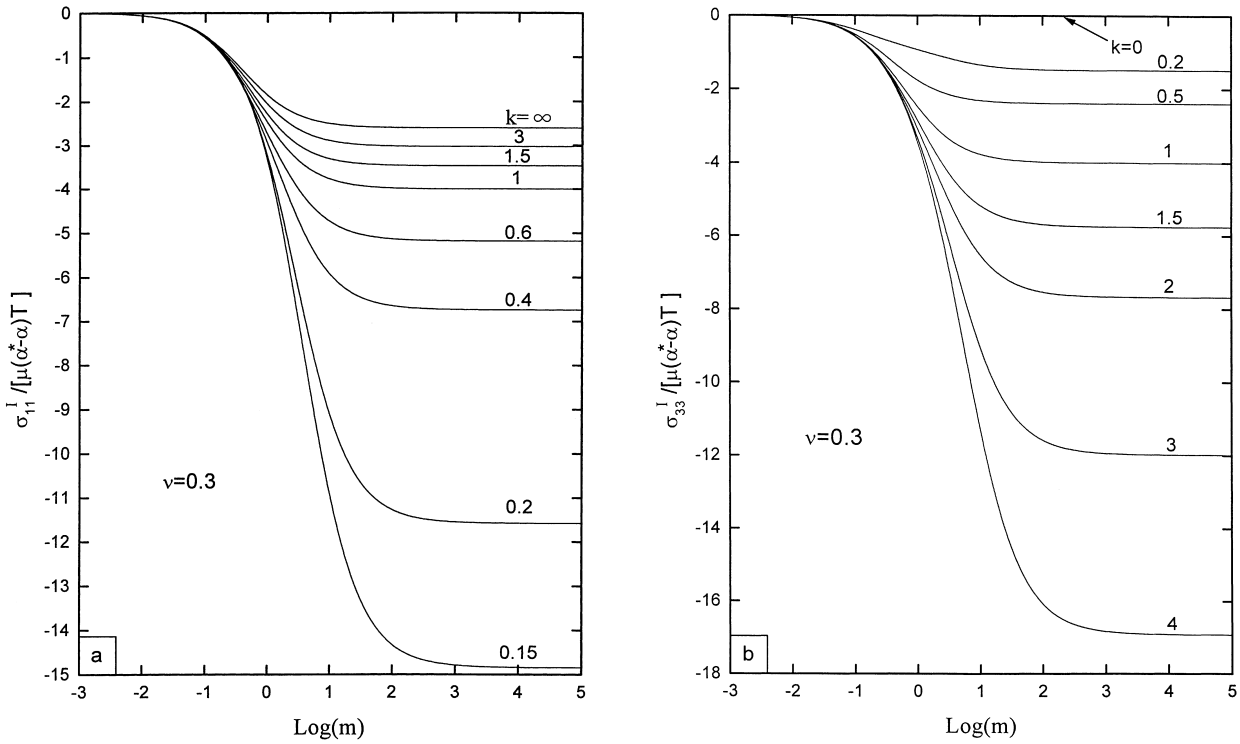

Fig. 1. (a) σ_{11}^{I} as a function of m for various values of k and (b) σ_{33}^{I}.

to be [15]

$$x_1 = f\csc\theta\sin\phi\cos\psi \tag{10a}$$

$$x_2 = f\csc\theta\sin\phi\sin\psi \tag{10b}$$

$$x_3 = f\cot\theta\cos\phi \tag{10c}$$

in which $f = \sqrt{a^2 - c^2} > 0$ is the focal length. The range of θ, ϕ, and ψ are

$$0 < \theta \le \frac{\pi}{2} \tag{11a}$$

$$0 \le \phi < \pi \tag{11b}$$

$$0 \le \psi < 2\pi \tag{11c}$$

Using the displacement-Newtonian potential relation established by Eshelby [1,2], we obtain the stress components outside the spheroid arising from the transformation strain e_{11}^{T}:

$$\sigma_{11}^{(1)} = -\frac{\mu e_{11}^{\mathrm{T}}}{4\pi(1-\nu)}\left\{3\Phi_{,11} + x_2\Phi_{,112} + \frac{1}{f^2}(a^2\Phi_{,11} + a^2x_3\Phi_{,113} - c^2\Phi_{,33} - c^2x_1\Phi_{,331})\right\} \tag{12a}$$

$$\sigma_{22}^{(1)} = \frac{\mu e_{11}^{\mathrm{T}}}{4\pi(1-\nu)}\{\Phi_{,11} + x_2\Phi_{,112} + 2\nu\Phi_{,33}\} \tag{12b}$$

$$\sigma_{33}^{(1)} = \frac{\mu e_{11}^{\mathrm{T}}}{4\pi(1-\nu)}\left\{2\nu\Phi_{,22} + \frac{1}{f^2}(a^2\Phi_{,11} + a^2x_3\Phi_{,113} - c^2\Phi_{,33} - c^2x_1\Phi_{,331})\right\} \tag{12c}$$

$$\sigma_{12}^{(1)} = \frac{\mu e_{11}^{\mathrm{T}}}{8\pi(1-\nu)}\left\{x_2\Phi_{,111} - x_1\Phi_{,222} - 2\Phi_{,12} + \frac{1}{f^2}(c^2x_1\Phi_{,332} - a^2\Phi_{,12} - a^2x_3\Phi_{,123})\right\} \tag{12d}$$

$$\sigma_{13}^{(1)} = \frac{\mu e_{11}^{\mathrm{T}}}{8\pi(1-\nu)}\left\{-x_1\Phi_{,223} - 4\Phi_{,13} + \frac{1}{f^2}(a^2x_3\Phi_{,221} - c^2x_1\Phi_{,223})\right\} \tag{12e}$$

$$\sigma_{23}^{(1)} = \frac{\mu e_{11}^{\mathrm{T}}}{8\pi(1-\nu)}\left\{x_2\Phi_{,113} + \frac{1}{f^2}(c^2\Phi_{,23} + c^2x_1\Phi_{,123} - a^2x_3\Phi_{,112})\right\} \tag{12f}$$

in which

$$\Phi = \frac{3V}{4f}\{\theta(3\cot^2\theta\cos^2\phi - \cot^2\theta + \cos^2\phi + 1) + \cot\theta(1 - 3\cos^2\phi)\} \tag{13a}$$

$$\Phi_{,11} = \frac{3V}{2f^3}\left\{\frac{\sin 2\theta(\csc^2\theta + \sin^2\phi\cos 2\psi)}{2g_0} - \theta\right\} \tag{13b}$$

$$\Phi_{,12} = \frac{3V}{4f^3g_0}\sin 2\theta\sin^2\phi\, 2\psi \tag{13c}$$

$$\Phi_{,13} = \frac{3V}{2f^3g_0}\sin\theta\sin 2\phi\cos\psi \tag{13d}$$

$$\Phi_{,112} = \frac{3V\cos\theta\sin\phi\sin\psi}{f^4 g_0}\left\{\sin^2\theta + \frac{(3-4\cos^2\theta)\sin^2\phi\cos^2\psi}{g_0} - \frac{4\cot^2\theta\sin^2\phi\cos^2\psi}{g_0^2}\right\} \tag{13e}$$

$$\Phi_{,113} = \frac{3V\sin^2\theta\cos\phi}{f^4 g_0}\left\{1 + \frac{(1-\cot^2\theta)\sin^2\phi\cos^2\psi}{g_0} - \frac{4\cos^2\theta\sin^2\phi\cos^2\psi}{g_0^2\sin^4\theta}\right\} \tag{13f}$$

$$\Phi_{,331} = \frac{3V\cos\theta\sin\phi\cos\psi}{f^4 g_0^3}\left\{\csc^2\theta\sin^2\phi - \sin^4\phi - 4\csc^2\theta\cos^2\phi\right\} \tag{13g}$$

$$\Phi_{,123} = -\frac{3V\sin2\phi\sin\phi\, sin2\psi}{4f^4 g_0^2}\left\{\cos2\theta + \frac{4\cot^2\theta}{g_0}\right\} \tag{13h}$$

$$g_0 = \csc^2\theta - \sin^2\phi \tag{13i}$$

$$V = \frac{4\pi a^2 c}{3} \tag{13j}$$

The subscript ',' represents the differentiation of the function with respect to a coordinate. Functions, $\Phi_{,22}$, $\Phi_{,23}$, $\Phi_{,221}$, $\Phi_{,223}$, and $\Phi_{,332}$ are obtained from $\Phi_{,11}$, $\Phi_{,13}$, $\Phi_{,112}$, $\Phi_{,113}$ and $\Phi_{,331}$ if $\cos\psi$ and $\sin\psi$ in Eqs. (13a), (13b), (13c), (13d), (13e), (13f), (13g), (13h), (13i) and (13j) are exchanged with each other. Since the Laplace equation of Newtonian potential, Φ, vanishes outside the spheroid, $\Phi_{,33}$ and $\Phi_{,111}$ are found to be

$$\Phi_{,33} = -\Phi_{,11} - \Phi_{,22} \tag{13k}$$

$$\Phi_{,111} = -\Phi_{,221} - \Phi_{,331} \tag{13l}$$

and $\Phi_{,222}$ and $\Phi_{,333}$ are obtained by a cyclic permutation of (123) in Eq. (13l).

The stress field $\sigma_{ij}^{(2)}$ in the matrix arising from the transformation strain, e_{22}^{T}, can be found from Eqs. (12a), (12b), (12c), (12d), (12e) and (12f) if subscripts, 1 and 2, are exchanged. The stress components in the matrix arising from the transformation strain, e_{33}^{T}, are

$$\sigma_{11}^{(3)} = \frac{\mu\nu e_{33}^{\mathrm{T}}}{2\pi(1-\nu)}\Phi_{,22} + \frac{\mu e_{33}^{\mathrm{T}}}{4\pi(1-\nu)f^2}\left\{a^2\Phi_{,11} + a^2x_3\Phi_{,113} - c^2\Phi_{,33} - c^2x_1\Phi_{,331}\right\} \tag{14a}$$

$$\sigma_{33}^{(3)} = \frac{\mu e_{33}^{\mathrm{T}}}{4\pi(1-\nu)f^2}\left\{(4c^2-a^2)\Phi_{,33} + c^2(x_1\Phi_{,331} + x_2\Phi_{,332}) + a^2x_3\Phi_{,333}\right\} \tag{14b}$$

$$\sigma_{12}^{(3)} = -\frac{\mu\nu e_{33}^{\mathrm{T}}}{2\pi(1-\nu)}\Phi_{,12} + \frac{\mu e_{33}^{\mathrm{T}}}{4\pi(1-\nu)f^2}\left\{a^2\Phi_{,12} + a^2x_3\Phi_{,123} - c^2x_1\Phi_{,332}\right\} \tag{14c}$$

$$\sigma_{13}^{(3)} = \frac{\mu e_{33}^{\mathrm{T}}}{8\pi(1-\nu)f^2}\left\{5c^2\Phi_{,13} + 2a^2x_3\Phi_{,331} + c^2(x_1\Phi_{,113} + x_2\Phi_{,223} - x_1\Phi_{,333})\right\} \tag{14d}$$

The components, $\sigma_{22}^{(3)}$ and $\sigma_{23}^{(3)}$, are found from $\sigma_{11}^{(3)}$ and $\sigma_{13}^{(3)}$ in Eqs. (14a) and (14d), if subscripts 1 and 2 are exchanged. The total stress components outside the spheroid are, then, given by

$$\sigma_{ij} = \sigma_{ij}^{(1)} + \sigma_{ij}^{(2)} + \sigma_{ij}^{(3)} \tag{15}$$

in which $\sigma_{ij}^{(1)}$ and $\sigma_{ij}^{(3)}$ are expressed in Eqs. (12a), (12b), (12c), (12d), (12e) and (12f) and Eqs. (14a), (14b), (14c) and (14d), respectively.

The above equations are also valid for the prolate spheroid coordinates, if f and θ are replaced by if and iθ where the range of θ is $(0,\infty)$ and $\mathrm{i} = \sqrt{-1}$. Therefore, the solution based on the oblate spheroid coordinates can be easily transformed to that based on the prolate spheroid coordinates. The conventional prolate spheroid coordinates (u_1,u_2,u_3) in terms of Cartesian coordinates (x_1,x_2,x_3) are [4,5,16]

$$x_1 = a\sinh u_1 \sin u_2 \cos u_3 \tag{16a}$$

$$x_2 = a\sinh u_1 \sin u_2 \sin u_3 \tag{16b}$$

$$x_3 = a\cosh u_1 \cos u_2 \tag{16c}$$

The oblate spheroid coordinates are obtained from the prolate spheroid coordinates, if $\sinh u_1$ and $\cosh u_1$ in Eqs. (16a), (16b) and (16c) are exchanged with each other. However, if a function cannot be explicitly expressed in terms of $\cosh u_1$ and $\sinh u_1$, it is very difficult to transform the function from the prolate spheroid coordinates to oblate spheroid coordinates, or vice versa. For example, u_1 and its polynomial can be expressed either by $\cosh^{-1}(\cosh u_1)$ or by $\sinh^{-1}(\sinh u_1)$, but they have no unique expression on $\sinh u_1$ and $\cosh u_1$. Sadowsky and Sternberg [4] and Edwards [5] used the prolate spheroid coordinates (u_1,u_2,u_3) to express the stress components instead of familiar Cartesian coordinates. Using Eqs. (16a), (16b) and (16c) with the Cartesian coordinates and spheroidal coordinates to express the stress components and functions, respectively, Shibata and Ono solved the elastic inclusion of a prolate spheroid [6] and an oblate spheroid [7], separately. In this paper, we use the new relation between the Cartesian coordinates and spheroidal coordinates, Eqs. (10a), (10b) and (10c) to replace Eqs. (16a), (16b) and (16c), and employ the Cartesian and spheroidal coordinates to express the stress components and functions. Then, the solution for prolate spheroid coordinates is readily transformed to that for oblate spheroidal coordinates.

Fig. 2 (a) shows the curves of σ_{11} outside the spheroid versus x_1 at $m = 2$ with various values of k. The σ_{11} increases monotonically with increasing x_1. Considering the points near the spheroid, the larger the slope of $|\mathrm{d}\sigma_{11}/\mathrm{d}x_1|$, the smaller the k. At the interface, σ_{11} is continuous along the x_1 direction regardless of k and m. Fig. 2(b) presents the relation of σ_{22} and x_1 with various values of k and $m = 2$. As shown in Fig. 2(b), σ_{22} decreases monotonically with increasing x_1 for $k \geq 0.5$ and increases to a maximum and then decreases with increasing x_1 for $k = 0.2$.

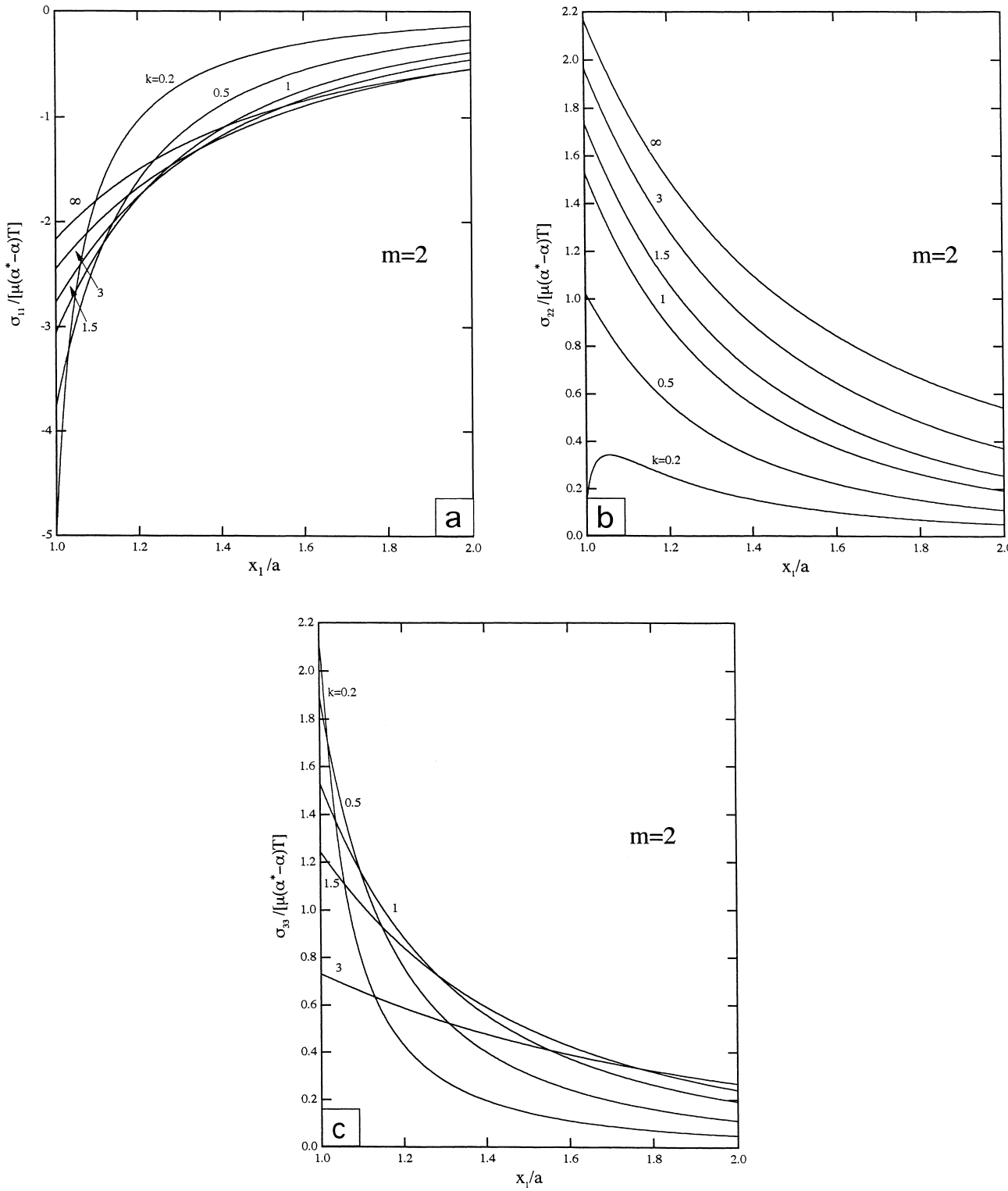

Fig. 2. The stresses outside the inclusion along x_1 axis at $m = 2$. (a) σ_{11} with various values of k; (b) σ_{22}; and (c) σ_{33}.

It is also seen that for a given x_1 and $m = 2$, σ_{22} increases with increasing k. Fig. 2(c) shows the σ_{33} as a function of x_1 with various values of k and $m = 2$. σ_{33} decreases with increasing k for $x_1 = a$, and the trend is opposite for large value of x_1. The slope of $d\sigma_{33}/dx_1$ drops at a greater rate when k is small. Note that for a rigid inclusion ($m = \infty$) with $k = 0.5$, σ_{33} increases to a maximum and then decreases with increasing x_1 (not shown in the above figures). Comparing Fig. 2(a–c), the longitudinal stress (σ_{11}) is compressive, and transverse stresses (σ_{22} and σ_{33}) are tensile along

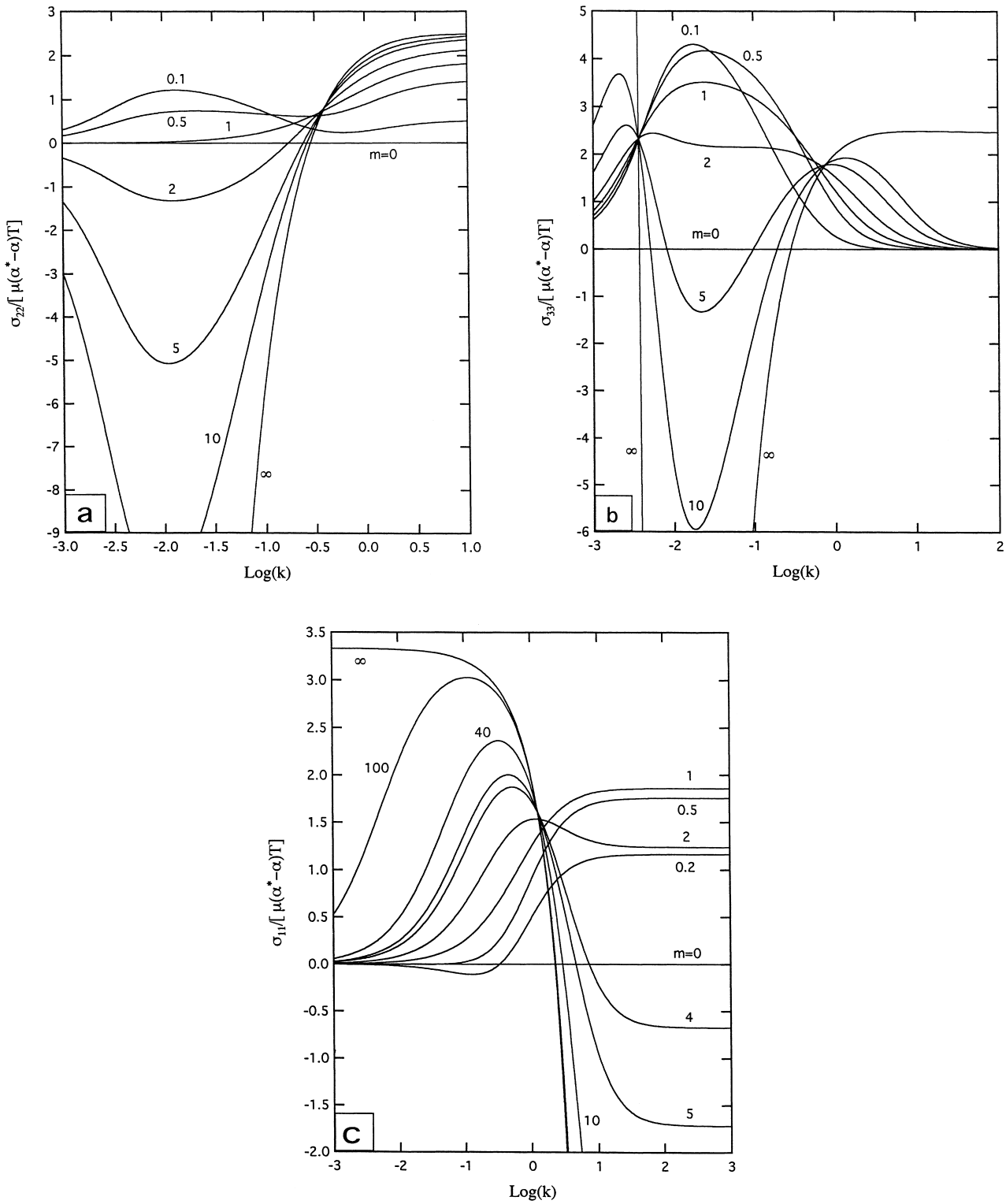

Fig. 3. Transverse stresses at the interface (a) σ_{22} at $x_1 = a$; (b) σ_{33} at $x_1 = a$; and (c) σ_{11} at $x_3 = c$.

the x_1 axis in the matrix. The curves of σ_{11} ($=\sigma_{22}$) and σ_{33} versus x_3 in the matrix are similar to those of σ_{22} (or σ_{33}) and σ_{11} along the x_1 axis, respectively.

In experimental studies [8], cracks were often observed along the interface between the inclusion and matrix. As stated in the preceding paragraph, the transverse stresses in the matrix (σ_{22} and σ_{33} along x_1 axis, σ_{11} and σ_{22} along x_3 axis) are always tensile and, generally, their magnitude decreases with increasing distance away from the spheroid, if $(\alpha - \alpha^*)T$ is greater than zero (but not always, for

example, the curve for $m = 2$ and $k = 0.2$, as shown in Fig. 2(b)). Among the three principal stresses, the maximum tensile stress is always located at the interface. The σ_{11} along the x_1 axis and σ_{33} along the x_3 axis are continuous across the interface, but σ_{22} and σ_{33} along the x_1 axis and σ_{11} ($=\sigma_{22}$) along the x_3 axis are not necessarily continuous at the interface. The σ_{11} ($= \sigma_{11}^{\mathrm{I}}$) at $x_1 = a$ and σ_{33} ($= \sigma_{33}^{\mathrm{I}}$) at $x_3 = c$ are shown in Fig. 1. We plot the stress components, σ_{22} and σ_{33}, at $x_1 = a$ and σ_{11} at $x_3 = \mathrm{c}$ in Fig. 3(a–c), respectively. It can be seen from Fig. 3(a) that σ_{22} is always positive for $k > 0.3$ regardless of m, and changes from negative to positive with increasing m for $k < 0.2$. It is always positive regardless of k for $m \leq 1$ and changes from negative to positive with increasing k for $m > 1$. As shown in Fig. 3(b), σ_{33} is always positive in the range of $-3 \leq \log(k) \leq 2$ for $m \leq 2$ and partly negative for $m \geq 5$. It increases to a maximum and then decreases with increasing k for $m \leq 1$, and oscillates with k for $m \geq 5$. All curves in Fig. 3(b) meet at point $k = 3.65 \times 10^{-3}$. σ_{11} at $x_3 = c$ is always positive regardless of k for $0.5 \leq m \leq 2$ (see Fig. 3(c)). It increases to a maximum, then decreases with increasing k, and finally reaches a plateau for $m \geq 4$. For $m \leq 2$, σ_{11} is of the S shape. Our results at points, (a,0,0) and (0,0,c), agree with those obtained by Edwards [5].

3. Summary and conclusions

Thermal stresses due to a spheroidal inclusion were analyzed based on the equivalent inclusion method proposed by Eshelby. A spheroidal inclusion in an infinite matrix is subjected to a temperature change T. A new relation between Cartesian coordinates and spheroid coordinates is established. Based on this relation, a given function expressed in prolate spheroid coordinates is easily transformed to that in oblate spheroid coordinates, or vice versa. Thus, the present solution is suitable for both prolate and oblate spheroidal inhomogeneities. The magnitude of the principal stress inside the spheroid increases with increasing m, the ratio of shear moduli of spheroid and matrix. The value of σ_{11}^{I} inside the spheroid increases with increasing k, the aspect ratio, but the trend for σ_{33}^{I} is opposite. The numerical results show that the maximum tensile stress is located at the interface between the spheroid and the matrix if $(\alpha^* - \alpha)T$ is greater than zero where α^* and α are the coefficients of thermal expansion of the spheroid and matrix, respectively. They are in good agreement with those reported in the literature.

Acknowledgements

One of us (SL) wishes to thank the National Science Council, Taiwan for financial support. The research was also sponsored by the Fossil Energy Advanced Research and Technology Development Materials Program and the division of Materials Science, US Department of Energy, under contract DE-AC05-84OR 21400 with Lockheed Martin Energy Research Corporation.

References

[1] J.D. Eshelby, Solid State Phys. 3 (1956) 89.
[2] J.D. Eshelby, Proc. Roy. Soc. London A241 (1957) 376.
[3] T. Mura, Micromechanics of Defects in Solids, 2nd ed., Kluwer Academic publishers, Dordrecht, 1987, p. 178.
[4] M.A. Sadowsky, E. Sternberg, J. Appl. Mech. 69 (1947) A191.
[5] R.H. Edwards, J. Appl. Mech. 73 (1951) 19.
[6] M. Shibato, K. Ono, J. Comp. Mater. 12 (1978) 132.
[7] M. Shibato, K. Ono, Acta Metall. 26 (1978) 921.
[8] R. Kolhe, C.Y. Hui, E. Ustundag, S.L. Sass, Acta Metall. Mater. 44 (1996) 279.
[9] N. Ramakrishnan, Acta Metall. Mater. 44 (1996) 69.
[10] E.U. Lee, Metall. Trans. 23A (1992) 2205.
[11] M.E. Fitzpatrick, M.T. Hutchings, J.E. King, D.M. Knowles, P.J. Withers, Metall. Mat. Trans. 26A (1995) 3191.
[12] M. Suery, C. Teodosiu, L.F. Menezes, Mat. Sci. Eng. A167 (1993) 97.
[13] W. Nowacki, Thermoelasticity, 2nd ed., Pergamon Press, Oxford, 1986, p. 71.
[14] J.K. Lee, D.M. Barnett, H.I. Aaronson, Metall. Trans. 8A (1977) 963.
[15] B.T. Chen, S. Lee, Proc. Natl. Sci. Counc. Part A, Phys. Sci. Eng. 22 (1998) 563.
[16] G. Arfken, Mathematical Methods for Physicists, Ch. 2, 2nd ed., Academic Press, New York, 1970.